Appl Water Sci (2013) 3:93–103
DOI 10.1007/s13201-012-0063-0

ORIGINAL ARTICLE

Carbon nanotubes-blended poly(phenylene sulfone) membranes for ultrafiltration applications

D. Lawrence Arockiasamy · Javed Alam · Mansour Alhoshan

Received: 29 February 2012 / Accepted: 3 September 2012 / Published online: 25 September 2012

Abstract Multi-walled carbon nanotubes (MWCNT) were carboxylated by a chemical method. Poly(phenylene sulfone) (PPSU), MWCNT and functionalized (carboxylated) MWCNT/poly(phenylene sulfone) (PPSU) blend membranes were synthesized via the phase-inversion method. The resultant membranes were then characterized by attenuated total reflectance Fourier transform infrared spectroscopy (ATR-FTIR), scanning electron microscopy (SEM), atomic force microscopy (AFM) and contact angle. The FMWCNT blend membranes appeared to be more hydrophilic, with higher pure water flux than did the pure PPSU and MWCNT/PPSU blend membranes. It was also found that the presence of multi-walled carbon nanotubes (MWCNTs) in the blend membranes was an important factor affecting the morphology and permeation properties of the membranes. The model proteins such as trypsin (20 kDa), pepsin (35 kDa), egg albumin (45 kDa) and bovine serum albumin (69 kDa) rejection experiments were carried out under identical operational conditions employing both PPSU and blend membranes. The membranes were also subjected to the determination of molecular weight cut-off (MWCO) using different molecular weights of proteins. During trypsin ultrafiltration, PPSU/MWCNT and PPSU/FMWCNT membranes showed a slower flux decline rate than did the PPSU membrane.

D. Lawrence Arockiasamy (✉) · J. Alam · M. Alhoshan
King Abdullah Institute for Nanotechnology, King Saud University, P.O. Box 2455, Riyadh 11451, Saudi Arabia
e-mail: ldass@ksu.edu.sa

Keywords Poly(phenylene sulfone) · Ultrafiltration · Carbon nanotubes · Nanocomposite · Blend membranes

Introduction

To date, polysulfone that is a family of thermoplastic polymers has been showing a continuous domination on the membranes of materials for separation technology due to low cost and ease of process in addition to thermal and chemical resistibility. However, these membranes comprising hydrophobic materials, which tend to suffer severe decreases in pure water flux, during operation caused by solute adsorption pore blocking and cake formation (Baker 2000). Membrane fouling, especially, is a serious problem in the case of protein separation because hydrophobic interactions between proteins and the membrane surface induce a non-selective and irreversible adsorption. Easily fouled membranes need frequent chemical cleaning and replacement of the membrane module, giving a sort lifetime, which leads to high utility costs (Pontie et al. 2007; Zularisam et al. 2007; Vrijenhoek et al. 2001; Shi et al. 2007). To circumvent the above drawbacks, it is well known that increasing the membrane hydrophilicity can effectively minimize membrane fouling (Zhao et al. 2010; Ran et al. 2011) though charged membranes can also be used to reduce membrane fouling (Mulder 1997). As such, methods such as surface graft polymerization, chemical grafting, and radiation-induced grafting have been developed in an attempt to increase the surface hydrophilicity of membranes (Deng et al.2009; Abu Seman et al. 2010).

Recently, the new types of membrane have been showing a promising role in improving existing membrane materials. For example, polymeric blend membranes, and polymeric nanocomposite membranes (organic–inorganic),

in which organic–inorganic membranes have great attractions for separation applications, because of their excellent mechanical strength and chemical resistance (Savage et al. 2009).

In addition, it is expected that such membranes will have the physicochemical stability of inorganic materials and the membrane-forming properties of polymers. In particular, nano-sized inorganic material-blended composite membranes are attractive because of their enhanced properties, such as high permselectivity, higher hydrophilicity, and enhanced fouling resistance (Liu et al. 2005; Shen et al. 2011; Lee et al. 2011). Literature reports have shown that there is a high potential for carbon nanotubes (CNTs) to improve the material properties of polymers (Kim et al. 2006, 2007; Peng et al. 2007a, b; Sharma et al. 2010; Aroon et al. 2010a, b, c; Cong et al. 2007). CNTs have an exceptionally high aspect ratio in combination with low density, and high strength and stiffness, which makes them a potential candidate as an effective reinforcing additive in polymeric materials.

Surprisingly, poly(phenylene sulfone) (PPSU) which is one the members of the polysulfone family, has superior physical and chemical properties compared to bisphenol-A-modified polysulfones. Only few researchers have studied the applicability of PPSU in fuel cell (Luisa Di Vona et al. 2006, 2008; Sgreccia et al. 2011; Hsiang Weng et al. 2008). However, not much attention was paid to PPSU for UF applications. Hence, the present investigation is aimed to study the utility of PPSU in ultrafiltration applications.

Carbon nanotube (MWCNT)-blended polysulfone ultrafiltration and microfiltration membranes were reported elsewhere. In view of literature, poly(phenylene sulfone) has not yet been used to prepare CNT-blended membranes for protein separation and water treatment. In this present investigation, multi-walled carbon nanotube/poly(phenylene sulfone) and functionalized multi-walled carbon nanotube/poly(phenylene sulfone) blend membranes were prepared and characterized, PPSU/MWCNT and PPSU/MWCNT blend membranes characterized in terms of pure water flux, water content and water contact angle. The enrichment of CNT in the surface of the membrane ascertained through Fourier transform infrared (FTIR) spectroscopy. The surface and cross-sectional morphology were analyzed by SEM. Furthermore, model proteins such as trypsin (20 kDa), pepsin (35 kDa), egg albumin (45 kDa) and bovine serum albumin (69 kDa) rejection experiments were carried out under identical operational conditions employing both the PPSU and blend membranes. The protein rejection efficiency and stable permeate flux were tested to compare the separation behavior of both the ultrafiltration membranes. Then, the fouling decline ratio was determined using trypsin as a model protein.

Experimental

Materials

Radel-5500 Poly (phenylene sulfone) was supplied by Solvay polymers. Analytical grade *N*-methylpyrrolidone (NMP) from Merck (I) Ltd was used as supplied as a solvent for the nanocomposite blend solution preparation. Carbon nanotubes were procured from Korean Carbon Nanomaterial Technology Co., Ltd. Anhydrous sodium monobasic phosphate and sodium dibasic phosphate heptahydrate were procured from Merck (I) Ltd and were used for the preparation of phosphate buffer solutions in the protein analysis. Proteins, viz., bovine serum albumin (BSA) (69 kDa), from Alpha Laboratories, India; egg albumin (EA) (45 kDa), from Merck (I) Ltd; pepsin (35 kDa) and trypsin (20 kDa) from BDH Chemicals Limited, was used as received. Deionized water was used throughout this study.

Fabrication of membranes

The blend solutions based on PPSU, PPSU/0.5 wt% MWCNT, PPSU/0.5 wt% FMWCNT (total polymer concentration = 17.5 wt%) were prepared by dissolving with different compositions in a solvent, NMP (80 wt%) under constant mechanical stirring at a moderate speed of rotation in a round bottomed flask for 4 h at 40 °C (before adding PPSU CNT and NMP were sonicated for 4 h to attain uniform dispersion of CNT in NMP). Multi-walled carbon nanotube (MWCNT) was carboxylated by chemical method as reported elsewhere. The homogeneous solution that was obtained was allowed to stand at room temperature for at least 1 day in an airtight condition to get rid of air bubbles. The method of preparation involved is the same as that of the "phase inversion" method employed in earlier works as reported by other researchers (Rahimpour and Madaeni 2007). The casting environment (relative humidity and temperature) was standardized for the preparation of membranes with better physical properties such as the homogeneity, thickness, and smoothness. The membrane-casting chamber was maintained at a temperature of 24 ± 1 °C and a relative humidity of 50 ± 2 %. The casting and gelation conditions were maintained constant throughout, because the thermodynamic conditions would largely affect the morphology and performance of the resulting membranes (Barth et al. 2000). The membranes were casted over a glass plate using a doctor blade. After casting, the solvent present in the cast film was allowed to evaporate for 30 s, and the cast film along with the glass plate was gently immersed in the gelation bath. After 2 h of gelation, the membranes were removed from the gelation bath and

washed thoroughly with distilled water to remove all NMP from the membranes. The membrane sheets were subsequently stored in distilled water, containing 0.1 % formalin solution to prevent microbial growth. Perkin Elmer attenuated total reflectance Fourier transform infrared spectroscopy (ATR) FTIR was employed for membrane surface characterization.

Compaction and pure water permeability test

The ultrafiltration experiments were carried out in a batch type, dead end cell (UF cell-Amicon, USA) with an internal diameter of 76 mm, fitted with Teflon-coated magnetic paddle. This cell was connected to a compressor with a pressure control valve and gauge through a feed reservoir. The thickness of the cast membrane was measured using a micrometer (Mitutoyo, Japan). The thickness of the membrane used in this study was 0.22 ± 0.02 mm. The prepared membranes were cut to the required size for use in the UF cell. The membranes were initially pressurized with distilled water at 414 kPa for 2 h. These pre-pressurized membranes were used in subsequent ultrafiltration experiments at 345 kPa. Membranes after compaction were subjected to pure water flux studies at a transmembrane pressure of 345 kPa. The flux was measured under steady-state flow. The pure water flux is determined as follows (Osada and Nakagawa 1992):

$$J_w = \frac{Q}{A.\Delta t}$$

where, J_w is the pure water flux (l m^{-2} h^{-1}), Q the quantity of pure water permeated (l) A the membrane area (m^2) and Δt is the sampling time (h).To determine membrane hydraulic resistance (R_m), the pure water flux of membranes was measured at different transmembrane pressures (ΔP) of 69, 138, 207, 276, 345 and 414 kPa, after compaction. The resistance of the membrane, R_m was evaluated from the slope of water flux versus transmembrane pressure difference (ΔP) using the following equation:

$$J_w = \frac{\Delta P}{R_m}$$

Water content and contact angle measurement

The water content of the membranes was determined by soaking the membranes in water for 24 h and weighing after mopping with blotting paper. The wet membranes were placed in a vacuum oven at 75 °C for 48 h and the dry weights were determined. From these values, the percentage water content was derived as follows (Tamura et al. 1981):

$$\text{Water content } (\%) = \frac{\text{wet sample weight } - \text{dry sample weight}}{\text{wet sample weight}} \times 100$$

Sessile drop method was employed to measure the contact angle of the membranes. The contact angles were measured at ten places and then average values were reported. Contact Angle Meter 110 VAC was employed to measure the contact angles.

Thermal stability of the membranes

The temperature of degradation was obtained by a thermo gravimetric analyzer with heating rate of 10 °C min^{-1} (Mettler, Model TA 3000) with a TG 50 thermo balance.

Morphological studies

The top surfaces of the CA/PPSU blend membranes were studied under a scanning electron microscope (SEM) (JEOL, Japan). The membranes were cut into pieces of various sizes and mopped with filter paper. These pieces were immersed in liquid nitrogen for 20–30 s and frozen. Frozen bits of the membranes were broken and kept in a desiccator. These dry membrane samples were used for SEM studies. The samples were gold-sputtered for producing electrical conductivity, and photomicrographs of the samples were taken under very high vacuum conditions operating between 5 and 10 kV, depending on the physical nature of the sample. Various SEM images were taken for top surface views of the polymeric membranes. In addition, atomic force microscopy (AFM) (using a Veeco Multi-Mode SPM with a Nanoscope V controller) was used to characterize the topography of membrane surfaces.

Protein separation

After mounting the compacted membrane in the UF cell, the chamber was filled with individual protein solutions and immediately pressurized with nitrogen gas to the desired level (345 kPa), which was maintained constant throughout the run. Proteins, i.e., BSA, EA, pepsin, and trypsin, were individually dissolved (0.1 wt%) in the phosphate buffer (0.05 M, pH 7.2) and used as standard solutions. The permeate was collected over measured time intervals and protein contents were analyzed with a spectrophotometer (Perkin Elmer) at the max of 280 nm. The permeate protein concentration was estimated using a UV–Vis spectrophotometer at a wavelength of 280 nm. The percentage of rejection was calculated using the formula:

$$SR\% = \left[1 - \frac{C_p}{C_f}\right] \times 100$$

where, C_p and C_f are the concentrations of permeate and feed solutions, respectively.

After compaction, 1 mg/ml trypsin concentration at pH 7 and with a phosphate buffer solution was used as ultrafiltration solution. The flux was collected over measured time intervals. Protein concentration was determined spectroscopically at 280 nm using a UV–visible spectrophotometer (Perkin Elmer). The flux during protein filtration was recorded until the constant flux was reached (J_p). Flux decline ratio (J_{FD}) value was calculated to reflect the fouling resistance ability of the membrane by the following equation:

$$J_{FD} = \left(1 - \frac{J_P}{J_W}\right) \times 100$$

Results and discussion

PPSU, PPSU/MWCNT and PPSU/FMWCNT membranes of 1 mm thickness were prepared by phase-inversion technique. Generally, hydrophilicity and surface structure are main factors, which have strong effects on the transport property of the membrane. The PPSU, PPSU/CNT nanocomposite membranes were characterized in terms of pure water flux, surface and cross-section morphology by SEM, contact angle by sessile drop method and also rejection percentage of proteins was studied and discussed in detail below.

FTIR (Fourier transform infrared spectroscopy)

Figure 1 shows the FTIR spectra of surfaces of the pure PPSU, PPSU/MWCNT and PPSU/FMWCNT blend membranes with 0.5 wt% CNTs. The PPSU/MWCNT blend membranes are noticeably different from the pure PPSU/FMWCNT membrane, with a new peak at 1,410 cm^{-1}, corresponding to the -OH vibration of carboxyl groups (Yuen et al. 2008). As such, it is thought that the blend membranes might be formed via hydrogen bonding interactions between the sulfonic groups of PPSU and the carboxylic groups of functionalized MWCNTs (Rong et al. 2010), as reported elsewhere.

Compaction and pure water permeability test

At constant operating pressure (414 kPa), the pure water flux of pure PPSU, PPSU/MWCNT and PPSU/MWCNT blend membranes upon compaction was measured for every 1 h. During compaction, the water flux was found to be high initially and declines gradually and reaches a steady state after 2–3 h of compaction. This initial decline in flux might be due to the fact that the membrane pores are being compacted leading to uniform pore size and steady-state water flux.

Membranes after compaction were subjected to a pressure of 345 kPa for the measurement of pure water flux. The flux was measured under steady-state flow (Osada and Nakagawa 1992). The values of pure water flux are presented in Fig. 2. Pure water flux of bare PPSU membrane at 345 kPa is 7.9 l m^{-2} h^{-1}. The addition of 0.5 wt% MWCNT to PPSU enhances the flux from 7.9 to 46.6 l m^{-2} h^{-1}. This drastic enhancement in flux might be due to the increase in segmental gap between the PPSU and CNT during membrane formation. In the case of PPSU/FMWCNT blend membranes, higher flux was observed in comparison with PPSU/MWCNT membranes. This enhancement in flux is due to addition of hydrophilic –COOH moieties in the blend membrane. Pure

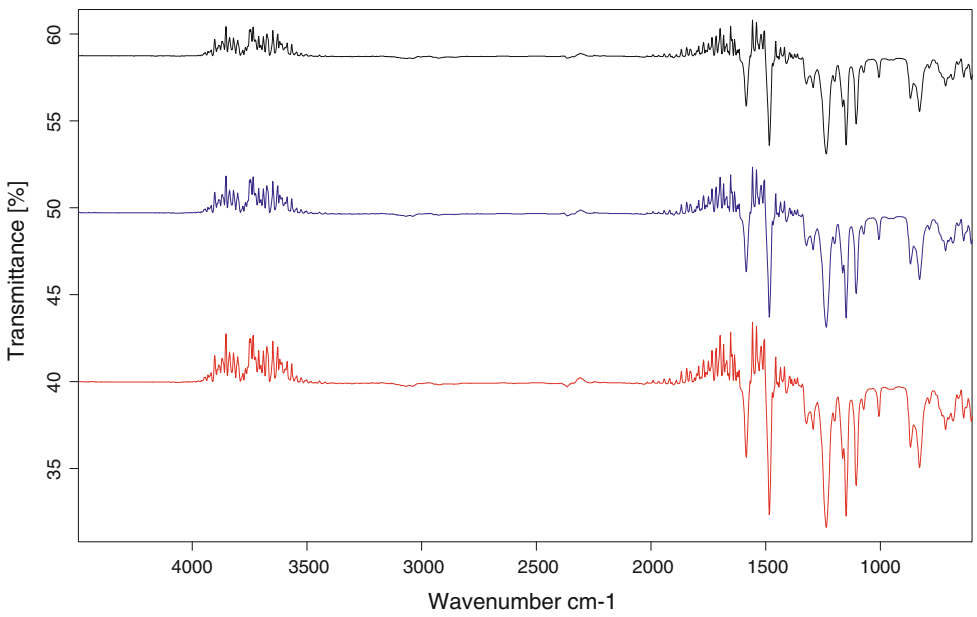

Fig. 1 ATR-IR spectrum of **a** PPSU, **b** PPSU/MWCNT, **c** PPSU/FMWCNT membranes

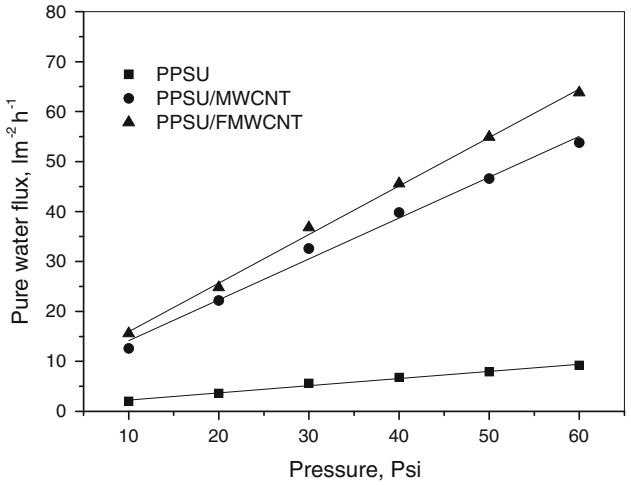

Fig. 2 Effect of pressure on PPSU, PPSU/MWCNT and PPSU/FMWCNT membranes

water flux for the PPSU/FMWCNT was found to be 56.9 l m^{-2} h^{-1} at 345 kPa. In order to determine the hydraulic resistance, the prepared membranes were subjected to different transmembrane pressures (TMP) from 69 to 414 kPa, and the corresponding pure water fluxes were measured. The plot of the pressure versus pure water flux gives a linear relationship and the inverse of the slope is the membrane hydraulic resistance. From Fig. 3, it is evident that the pure water flux increased with increased operating pressure. The higher R_m exhibited by 100 % PPSU membrane, i.e., 6.98. Addition of 0.5 wt% MWCNT into PPSU the hydraulic resistance decreased from 6.98 to 1.22 kPa/l m^{-2} h^{-1}. This is due to PPSU/MWCNT membrane being more hydrophilic and less crystalline compare to PPSU membranes. The R_m value for PPSU/FMWCNT was found to be 1.03 kPa/l m^{-2} h^{-1}, this slight decrease in R_m value due to incorporation of –COOH group in MWCNT resulting in higher permeate water flux.

Water content and contact angle

Contact angle measurement of membranes and water content is considered to be an important parameter for membrane characterization, since the pure water flux of the membrane can be predicted based on these results. Water content of the membranes is an indirect indication of the hydrophilicity and flux behavior of membranes. Membranes were thoroughly washed with distilled water before estimation of water content. The pure PPSU membrane in absence of CNT was found to have water content of 60 %. In the case of PPSU/MWCNT nanocomposite membrane the water content was increased; it was found to be 70 %. Addition of MWCNT increased the immiscible nature of blend due to poor adhesion properties between PPSU and CNT. Further, this leads to increase in void volume of membrane, which results in the formation of bigger size pores. In the case of PPSU/FMWCNT blend membranes, higher water content was observed in comparison with PPSU/MWCNT membranes. This enhancement in water content is due to addition of hydrophilic –COOH moieties in the blend membrane. Water content for the PPSU/FMWCNT was found to be 73 %.

Contact angle measurement was performed on PPSU, PPSU/MWCNT and PPSU/FMWCNT films using a sessile drop method. The change in the contact angle of the films was measured by dropping the water on the membrane surface. The contact angles were measured at ten places and then average values were reported. As shown in Fig. 4, the PPSU membrane had the highest contact angle (76°), corresponding to the lowest hydrophilicity. The contact angle decreases with the addition 0.5 wt% MWCNT in this

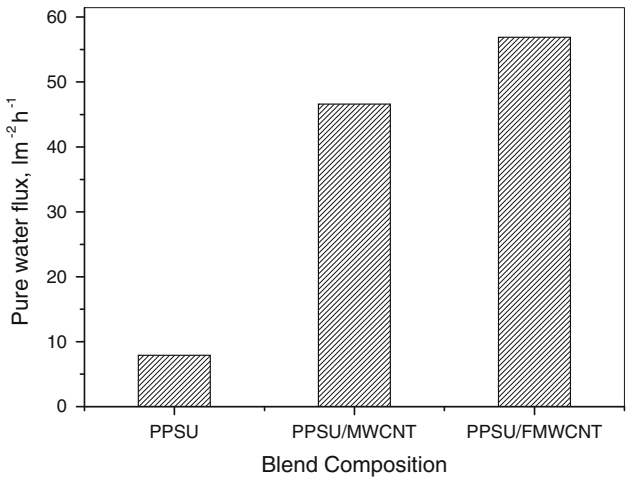

Fig. 3 Pure water flux at 345 kPa

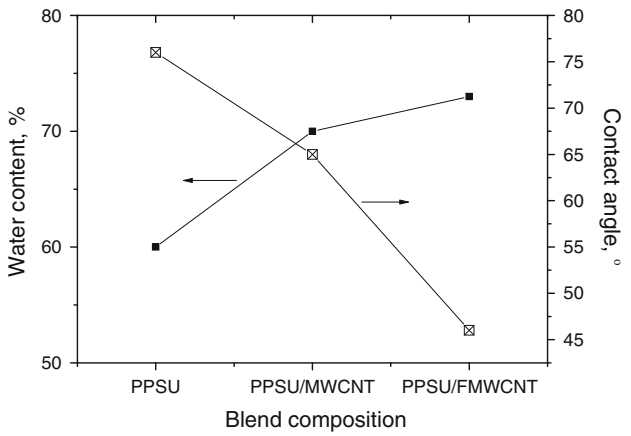

Fig. 4 Water content and contact angle of PPSU, PPSU/MWCNT and PPSU/FMWCNT membranes

blend due to increase of hydrophilicity. In the case of PPSU/FMWCNT blend membranes, lower contact angle was observed in comparison with PPSU/MWCNT membranes. The decrease in the water contact angle of modified membranes implies that a polar surface was obtained by increasing the –COOH group and the hydrophilicity of PPSU/FMWCNT membranes was improved by increasing the average polarity of the blend. Therefore, it was proposed that the carboxylated membranes absorb more permeate into the membrane and thus enhance the flux rate. The static contact angles of the PPSU/MWCNT and PPSU/FMWCNT are 65° and 45°, respectively.

Thermal stability of membranes

The thermal stability of pure PPSU, PPSU/MWCNT and PPSU/FMWCNT films were investigated by TGA. The experiment was run from 20 to 800 °C at a heating rate of 10 °C min^{-1} under nitrogen atmosphere. The thermal degradation behaviors of PPSU, PPSU/MWCNT and PPSU/FMWCNT blend membranes are shown in Fig. 5. It is seen that from Fig. 5 the initial degradation above 400 °C may be attributed to loss of sulfone content in poly(phenylene sulfone), while the decomposition above 500 °C may be assigned to degradation of polymer chain. The thermal behavior of PPSU/MWCNT revealed that slight enhancement of degradation temperature on comparison with bare PPSU. Similar trend was also observed for PPSU/FMWCNT blend nanocomposite membranes in the initial TGA; however, after at 450 °C the thermal stability is slightly reduced due to decomposition of –COOH started after 450 °C. Thermal stability studies reveal that nanocomposite membranes shows higher thermal stability than bare PPSU membranes.

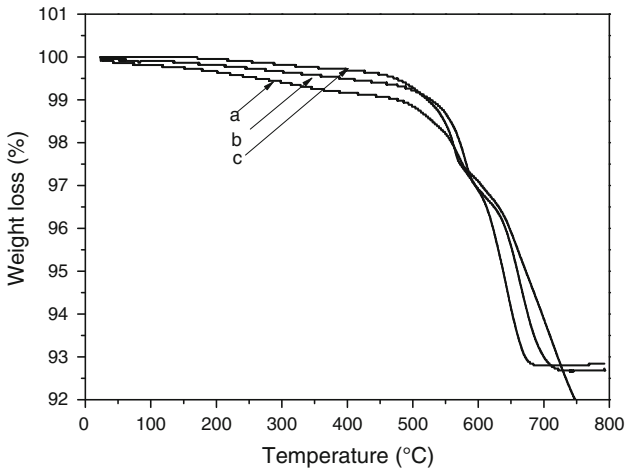

Fig. 5 TGA curve for PPSU, PPSU/MWCNT and PPSU/FMWCNT membranes

Morphological studies

The surface and cross-section structure of a flat sheet, ultrafiltration membrane, is the most critical part, helping to identify the role of the membrane in the mechanism of permeation and rejection. SEM is important for the determination of morphology of the membranes. To attain high-performance membranes for specific applications, it is essential to manipulate the morphological structures of the membranes (Malaisamy et al. 2002). Hence, the morphological studies of the blend membranes were made using SEM. The SEM micrographs of top surface of PPSU, PPSU/MWCNT and PPSU/FMWCNT blend are shown in Fig. 6a–c. A good and smooth surface was observed for all three membranes. Cross sections of PPSU, PPSU/MWCNT and PPSU/FMWCNT blend are shown in Fig. 6d–f. PPSU and PPSU/MWCNT membranes showed a typical asymmetric membrane structure with a dense top layer, a porous sub-layer, and fully developed macropores at the bottom. Nevertheless, PPSU/FMWCNT membrane reveals that the formation of macropores was suppressed by the addition of FMWCNTs into the membrane structure. PPSU/FMWCNT membranes showed an asymmetric membrane structure with a dense top layer, a porous middle layer, and followed spongy sub-layer. This may be due to incorporation of –COOH group in the PPSU blend changing the thermodynamic behavior during the gelation resulting alters the membrane cross section.

Atomic force microscopy is an excellent tool for measuring the external surface roughness of the polymeric membranes, which may significantly visualize fouling behavior of membranes. 3D and phase AFM images for pure PPSU, PPSU/MWCNT and PPSU/FMWCNT were taken and shown in Fig. 7a–d. From AFM images, changes in membranes roughness were clearly observed. Functional nanocomposites membranes had better surface compared to PPSU and PPSU/MWCNT nanocomposites membranes. It might be because of a good compatibility of functional FMWNCT with polysulfone matrix due to acid functional group. Due to smooth surface, PPSU/FMWCNT blend membrane was less prone to fouling compared to pristine PPSU membranes. Therefore, inclusion of FMWCNT into PPSU membrane may be considered as one of the potential solutions to alter the surface roughness properties.

Protein rejection studies

The rejection of the proteins BSA, EA, pepsin and trypsin were attempted individually with the prepared membranes. Initially, a protein of low-molecular weight, trypsin, was used for the UF experiments because we expected the use of a high molecular weight protein at the beginning would spoil the originality of the pores for the separation and comparison of

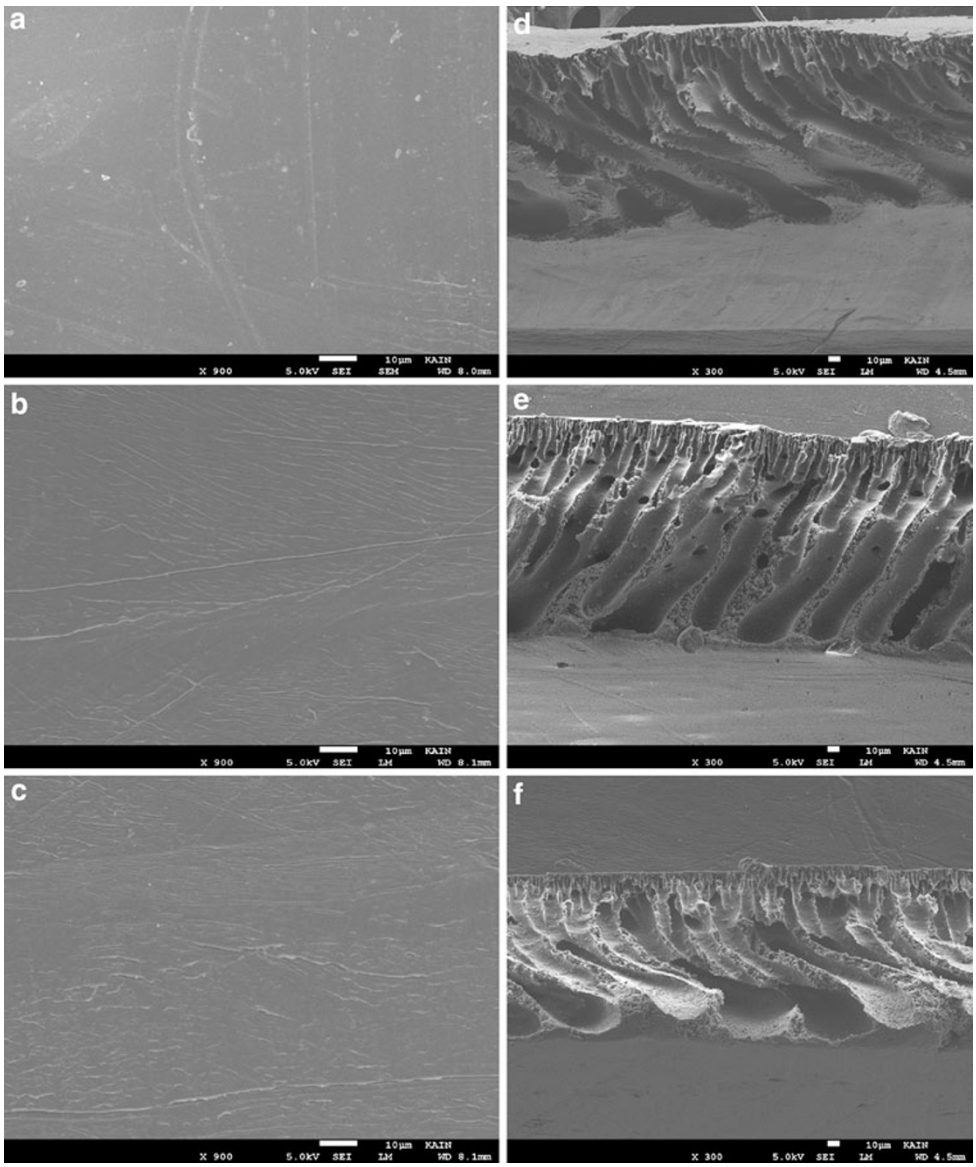

Fig. 6 SEM images of surface: **a** PPSU, **b** PPSU/MWCNT, **c** PPSU/FMWCNT. Cross section: **d** PPSU, **e** PPSU/MWCNT, **f** PPSU/FMWCNT membranes

low-molecular weight proteins. The interaction of the solutes with the membranes results in adsorptive fouling and interferes with the performance of the membranes. The pH of the individual feed solutions was kept constant at 7.2, since a change in pH may increase the adsorptive fouling of the membranes (Brinck et al. 2000). Furthermore, intermolecular forces between protein molecules and membranes will predominate and affect the efficiency of membranes if the pH of the solution changes (Koehler et al. 2000). All the experiments were carried out at least three times to observe the reproducibility. The results provided are the average of three values; the deviations between each value were negligibly small. It is seen from the Fig. 8 pure PPSU membrane exhibited rejections of 99 % for BSA and EA. The higher rejection of BSA and EA is due to its larger size compared with pepsin and trypsin. The rejection percentage of pepsin and trypsin is 97 and 90 %, respectively. The PPSU/MWCNT blend nanocomposite membrane exhibits slightly less rejection compared to bare PPSU membrane. The structural change occurred with the addition of MWCNT in PPSU polymer moiety and increases the pore size of the nanocomposite membrane. PPSU/FMWCNT nanocomposite membrane resulted in slightly lesser rejection of all protein compared to PPSU/MWCNT membrane. This decrease in rejection is due to carboxylated CNT altering the membrane surface and inside the membrane structure. The increased pore size is accredited to the partial miscibility of PPSU and CNT. The increase in pore size of blend membranes with increasing CNT content in the blend membranes was also confirmed by SEM.

The permeate flux of protein solution is essential to specify the product rate and predict the economics of the

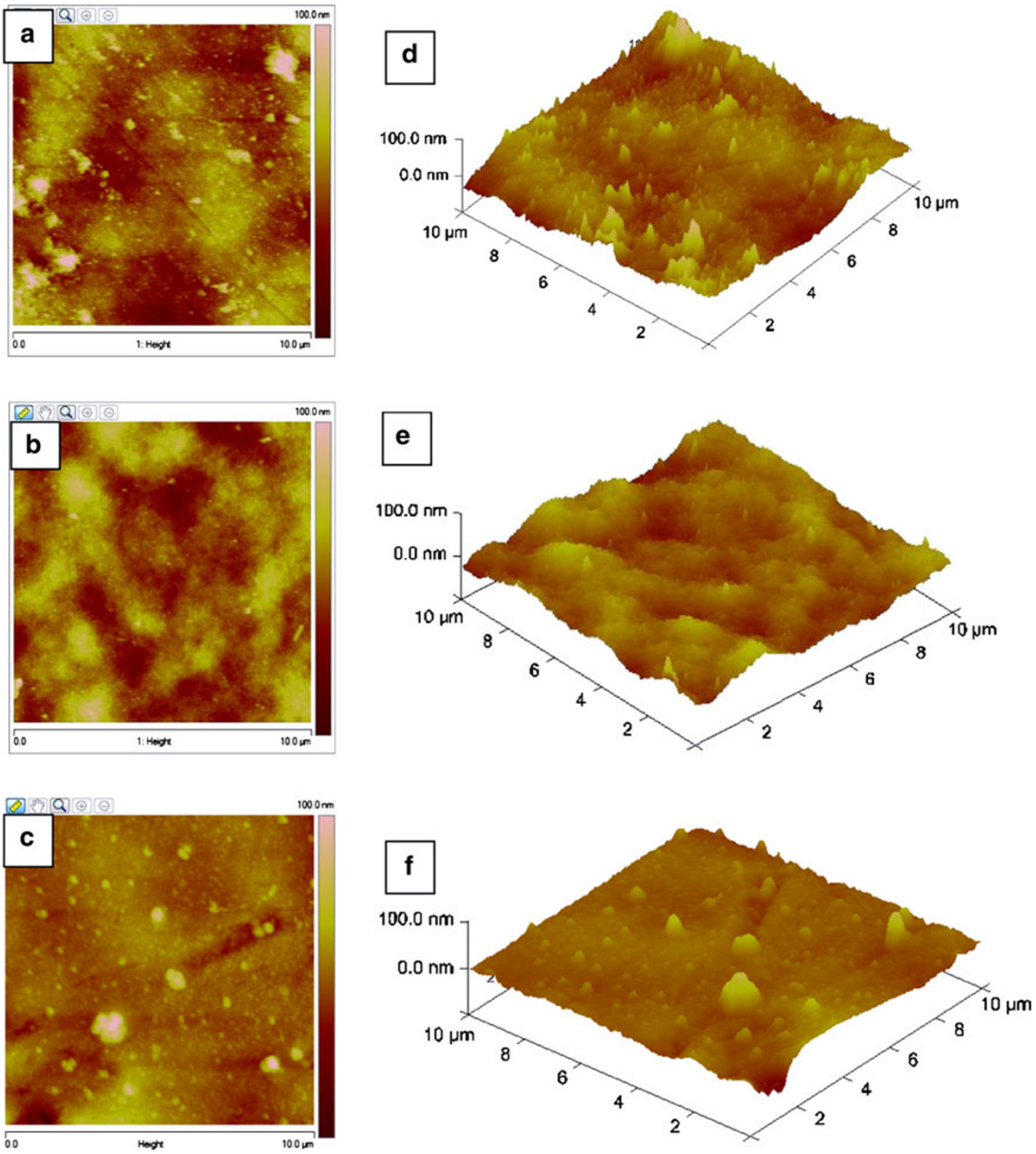

Fig. 7 AFM images for pure PPSU and PPSU/FMWCNT membranes

membrane process. The aqueous protein solution permeate fluxes were measured simultaneously during rejection experiments for PPSU, PPSU/MWCNT and PPSU/FMWCNT membranes. The pure (100 %) PPSU membrane offered a lower flux value of 2.6 l m^{-2} h^{-1} for BSA and a higher value of 3.8 l m^{-2} h^{-1} for trypsin. When the 0.5 wt% MWCNT was added, the flux of BSA increased from 23.6 to 41.1 l m^{-2} h^{-1} BSA as shown in Fig. 9. In the case of PPSU/FMWCNT system, the protein flux values are 32.6, 36.9, 42.7 and 52.6 for BSA, EA, pepsin and trypsin, respectively. This enhancement in flux upon increase of FMWCNT might lead to the higher hydrophilicity by means of carboxylation. MWCO is a pore characteristic of membranes and is related to rejection for a given molecular weight of a solute. The molecular weight has a linear relationship with the pore radius or pore size of a membrane (Mahendran et al. 2004). In general, the MWCO of a membrane is determined by the identification of an inert solute, which has the lowest molecular weight and has a solute rejection of 80–100 % in steady-state UF

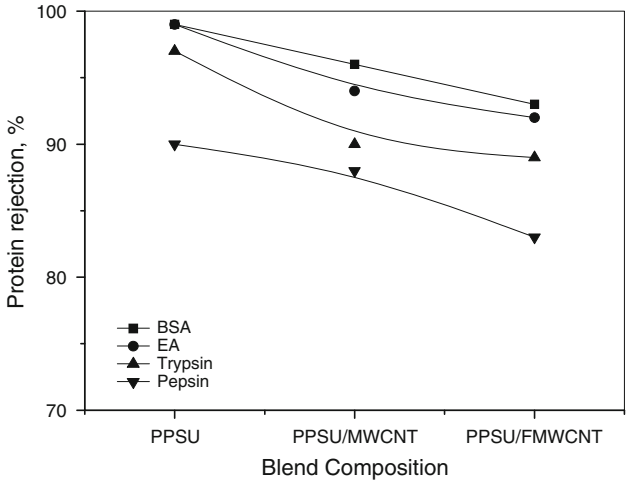

Fig. 8 Protein rejection of PPSU, PPSU/MWCNT and PPSU/FMWCNT membranes

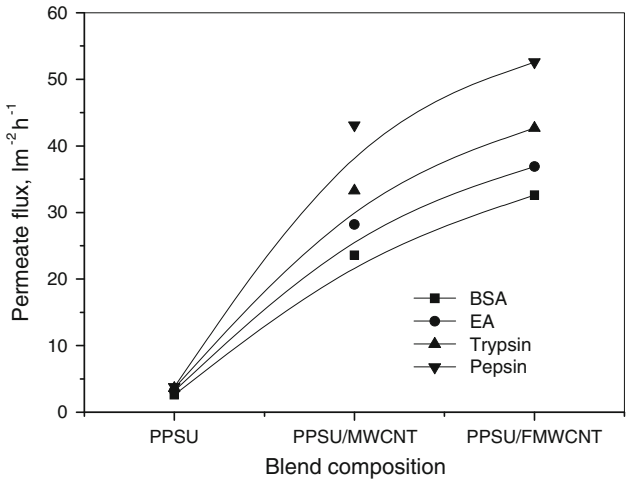

Fig. 9 Protein permeates flux of PPSU, PPSU/MWCNT and PPSU/FMWCNT membranes

experiments (35). This study reveals that almost all the three membranes exhibited the MWCO value around 20–30 kDa.

Antifouling properties

Figure 8 shows the effect of MWCNT and FMWCNT on the protein flux of the PPSU membranes. Compacted PPSU, PPSU/MWCNT and PPSU/FMWCNT membranes were employed for ultrafiltration of the BSA solution. Before ultrafiltration of BSA solution, the blend membranes were cleaned with pure water for an hour, which shows that there is no significant change in the pure water flux, as shown in Fig. 10. The flux decreased dramatically at the initial operation of BSA solution ultrafiltration due to protein adsorption or convective deposition. It is proposed

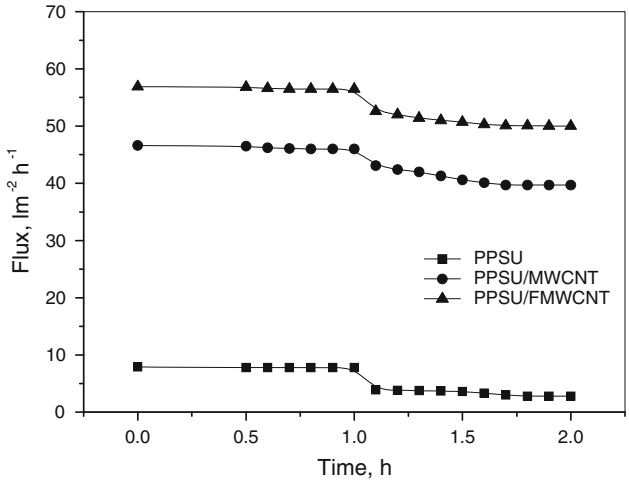

Fig. 10 Effect of CNT and FCNT in PPSU membrane on the protein permeates flux

that some protein molecules in the feed deposit or adsorb on the membrane surface (cake formation), causing a drop in the first few minutes of operation. Under constant pressure, the effects of membrane fouling and concentration polarization are usually observed by considerable decline in permeate flux with time. In the present work, the concentration polarization was minimized because of high molecular weight BSA molecules and rigorous stirring near the membrane surface (Lawrence Arockiasamy et al. 2009). Therefore, the flux decline of the membranes was mostly caused by membrane fouling. Flux decline ratio (R_{FD}) value is introduced to reflect the fouling resistance ability of the membrane; a lower value of R_{FD} means a higher fouling resistance ability of the membrane. For the PPSU and PPSU/MWCNT, PPSU/FMWCNT blend membranes, the R_{FD} values were 64, 14, and 11 (Fig. 9), respectively. It indicated that the fouling resistance increased with an addition of MWCNT in the casting solution. The lowest R_{FD} value was observed for PPSU/FMWCNT membrane. This is probably due to the more hydrophilic –COOH group enrichment of the membrane surface, which is consistent with contact angle measurements of blend membrane surfaces.

Conclusions

Poly(phenylene sulfone) membranes were successfully modified by adding MWCNT and carboxylated MWCNT for the formation of the blend membranes, where MWCNT and FMWCNT resulted in higher separation figures of merit including with water flux and water content and lower hydraulic resistance. The addition of MWCNT and FMWCNT also slightly altered the molecular weight

cut-off (MWCO), membrane structure and the mechanical properties of the membranes. The improved surface hydrophilicity, due to surface enrichment of –COOH content, endowed the PPSU/FMWCNT blend membranes with significantly enhanced protein adsorption resistance. We observed that the incorporation of the hydrophilic MWCNT and FMWCNT blend membranes played a major role in improving the flux and performance characteristics of membranes.

References

Abu Seman MN, Khayet M, Bin Ali ZI, Hilal N (2010) Reduction of nanofiltration membrane fouling by UV-initiated graft polymerization technique. J Membr Sci 355:133–141

Aroon MA, Ismail AF, Montazer Rahmati MM, Matsuura T (2010a) Effect of raw multi wall carbon nanotubes on morphology and separation properties of polyimide membranes. Sep Sci Technol 45:2287–2297

Aroon MA, Ismail AF, Montazer Rahmati MM, Matsuura T (2010b) Effect of chitosan as a functionalization agent on the performance and separation properties of polyimide/multi-walled carbon nanotubes mixed matrix flat sheet membranes. J Membr Sci 364:309–317

Aroon MA, Ismail AF, Matsuura T, Montazer Rahmati MM (2010c) Performance studies of mixed matrix membranes for gas separation: a review. Sep Purif Technol 75:229–242

Baker RW (2000) Membrane technology and applications, 2nd edn. John Wiley & Sons Ltd, Menlo Park

Barth C, Gonclaves MC, Pires ATN, Roeder J, Wolf BA (2000) Asymmetric polysulfone and polyethersulfone membranes: effects of thermodynamic conditions during formation on their performance. J Membr Sci 169:287–299

Brinck J, Jansson A, Jonsson B, Lindau J (2000) Influence of pH on the adsorption fouling of ultrafiltration membranes by fatty acid. J Membr Sci 164:187–194

Cong H, Zhang J, Radosz M, Shen Y (2007) Carbon nanotube composite membranes of brominated poly(2,6-diphenyl-1,4-phenylene oxide) for gas separation. J Membr Sci 294:178–185

Deng J, Wang L, Liu L, Yang W (2009) Developments and new applications of UV-induced surface graft polymerizations. Prog Polym Sci 34:156–193

Hsiang Weng T, Hsin Tseng H, Yen Wey M (2008) Preparation and characterization of PPSU/PBNPI blend membrane for hydrogen separation. Int J Hydrogen Energ 33:4178–4182

Kim S, Pechar TW, Marand E (2006) Poly(imide siloxane) and carbon nanotube mixed matrix membranes for gas separation. Desalination 192:330–339

Kim S, Jinschek JR, Chen H, Sholl DS, Marand E (2007) Scalable fabrication of carbon nanotube/polymer nanocomposite membranes for high flux gas transport. Nano Lett 7:2806–2811

Koehler JA, Ulbricht M, Belfort MG (2000) International forces between a protein and a hydrophilic modified polysulfone film with relevance to filtration. Langmuir 16:10419–10427

Lawrence Arockiasamy D, Nagendran A, Shobana KH, Mohan D (2009) Preparation and characterization of cellulose acetate/aminated polysulfone blend ultrafiltration membranes and their application studies. Sep Sci Technol 44:398–421

Lee KP, Arnot TC, Mattia D (2011) A review of reverse osmosis membrane materials for desalination—development to date and future potential. J Membr Sci 370:1–22

Liu J, Xu T, Fu Y (2005) Fundamental studies of novel inorganic–organic charged zwitterionic hybrids: 2. Preparation and characterizations of hybrid charged zwitter ionic membranes. J Membr Sci 252:165–173

Luisa Di Vona M, Alessandra DE, Marani D, Trombetta M, Traversa E, Licoccia S (2006) SPEEK/PPSU-based organic–inorganic membranes: proton conducting electrolytes in anhydrous and wet environments. J Membr Sci 279:186–191

Luisa Di Vona M, Luchetti L, Spera GP, Sgreccia E, Knauth P (2008) Synthetic strategies for the preparation of proton-conducting hybrid polymers based on PEEK and PPSU for PEM fuel cells. C R Chim 11:1074–1081

Mahendran R, Malaisamy R, Mohan D (2004) Cellulose acetate and polyethersulfone blend ultrafiltration membranes. Part I. Preparation and characterizations. Polym Adv Technol 15:149–157

Malaisamy R, Mahendran R, Mohan D (2002) Cellulose acetate and polysulfone blend ultrafiltration membranes-II pore statistics, molecular weight cutoff and morphological studies. J Appl Polym Sci 84:430–444

Mulder M (1997) Basic principles of membrane technology, 2nd edn. Kluwer Academic Publishers, The Netherlands

Osada V, Nakagawa I (1992) Membrane science and technology. Marcel Dekker, New York

Peng F, Pan F, Sun H, Lu L, Jiang Z (2007a) Novel nanocomposite pervaporation membranes composed of poly(vinyl alcohol) and chitosan-wrapped carbon nanotubes. J Membr Sci 300:13–19

Peng F, Hu C, Jiang Z (2007b) Novel poly(vinyl alcohol)/carbon nanotube hybrid membranes for pervaporation separation of benzene/cyclohexane mixtures. J Membr Sci 297:236–242

Pontie M, Thekkedath A, Kecili K, Habarou H, Suty H, Crou JP (2007) Membrane autopsy as a sustainable management of fouling phenomena occurring in MF, UF and NF processes. Desalination 204:155–169

Rahimpour A, Madaeni SS (2007) Polyethersulfone (PES)/cellulose acetate phthalate (CAP) blend ultrafiltration membranes: preparation, morphology, performance and antifouling properties. J Membr Sci 305:299–312

Ran F, Nie S, Zhao W, Li J, Su B, Sun S, Zhao C (2011) Biocompatibility of modified polyethersulfone membranes by blending an amphiphilic triblock co-polymer of poly(vinyl pyrrolidone)-b-poly(methyl methacrylate)-b-poly(vinyl pyrrolidone). Acta Biomater 7:3370–3381

Rong C, Ma G, Zhang S, Song L, Chen Z, Wang G, Ajayan PM (2010) Effect of carbon nanotubes on the mechanical properties and crystallization behavior of poly(ether ether ketone). Compos Sci Technol 70:380–386

Savage N, Diallo M, Duncan J, Street A, Sustich R (2009) Nanotechnology application for clean water, 1st edn. William Andrew Inc., New York

Sgreccia E, Di Vona ML, Knauth P (2011) Hybrid composite membranes based on SPEEK and functionalized PPSU for PEM fuel cells. Int J Hydrogen Energ 36:8063–8069

Sharma A, Tripathi B, Vijay YK (2010) Dramatic improvement in properties of magnetically aligned CNT/polymer nanocomposites. J Membr Sci 361:89–95

Shen J, Ruan H, Wu L, Gao C (2011) Preparation and characterization of PES–SiO_2 organic–inorganic composite ultrafiltration membrane for raw water pretreatment. Chem Eng J 168:1272–1278

Shi Q, Su Y, Zhu S, Li C, Zhao Y, Jiang Z (2007) A facile method for synthesis of pegylated polyethersulfone and its application in

fabrication of antifouling ultrafiltration membrane. J Membr Sci 303:204–212

Tamura M, Uragami T, Sugihara M (1981) Studies on synthesis and permeabilities of special polymer membranes, CA30. Ultrafiltration and dialysis characteristics of cellulose nitrate poly (vinylpyrrolidone) polymer blend membranes. Polymer 22:829–835

Vrijenhoek EM, Hong S, Elimelech M (2001) Influence of membrane surface properties on initial rate of colloidal fouling of reverse osmosis and nanofiltration membranes. J Membr Sci 188:115–128

Yuen SM, Ma CCM, Chiang CL, Teng CC (2008) Morphology and properties of aminosilane grafted MWCNT/polyimide nanocomposites. J Nanomater 2008:1–15

Zhao YH, Wee KH, Bai R (2010) Highly hydrophilic and low-protein-fouling polypropylene membrane prepared by surface modification with sulfobetaine-based zwitterionic polymer through a combined surface polymerization method. J Membr Sci 362:326–333

Zularisam AW, Ismail AF, Salim MR, Sakinah M, Ozaki H (2007) The effects of natural organic matter (NOM) fractions on fouling characteristics and flux recovery of ultrafiltration membranes. Desalination 212:191–208